PROCEEDINGS of the
23rd International Congress on Acoustics

9 to 13 September 2019 in Aachen, Germany

Lumped parameter model and Monte Carlo simulation to study middle ear uncertainties

Lucas LOBATO(1), Stephan PAUL(2), Júlio A. CORDIOLI(3)

(1)Acoustic and Vibration Laboratory, Federal University of Santa Catarina, Brazil. lucas.lobato@lva.ufsc.br

(1)Acoustic and Vibration Laboratory, Federal University of Santa Catarina, Brazil. stephan.paul@ufsc.br

(1)Acoustic and Vibration Laboratory, Federal University of Santa Catarina, Brazil. julio.cordioli@ufsc.br

Abstract

Several mathematical models of the human middle ear have been developed throughout the last 70 years for different purposes. Although the experimental data of the dynamical behavior of the middle ear show a large dispersion, only deterministic models have been proposed in the literature. This work aims to develop a probabilistic model of the human middle ear to study its dynamic behavior uncertainties. Then, a coupled lumped parameter and analytical model is combined to Monte Carlo simulations (MCS). The parameters of the deterministic model was fitted to match the stapes velocity to one experimental results. Then, the input parameters were modeled with Gaussian probability density functions in the MCS. It was observed the uncertainty of the natural frequencies increases with the mode order. Also, the dispersion seen experimentally could not be reproduced defining the standard deviation (StD) of the input parameters as 20% of the mean value. Therefore, the StD of the input parameters was increased up to 30%, 40% and 50% of the mean values. Results suggest the StD should be defined separately for each input parameter in order to reproduced the experimental dispersion. At last, next steps are set for improvements in the proposed probabilistic approach. Keywords: Middle ear, Biomechanics, Uncertainties, Probabilistic model

1 INTRODUCTION

The middle ear is a biomechanical system that composes the peripheral auditory system of mammals together with the outer and inner ears. The middle ear is mainly composed of a complex fibrous membrane called tympanic membrane (TM), an ossicular chain comprising three tiny bones (malleus, incus and stapes), two synovial joints and various soft tissues such as ligaments, tendons and muscles [1]. Two functions are assigned to the physiological working of the middle ear. At first, the middle ear matches the several different impedances of the outer and inner ears, improving the transmission of the sound energy between these two systems. Secondly, the middle ear protects the inner ear against high static pressures and high sound stimuli through passive and active working [2].

For a proper understand of the middle ear mechanics under healthy and pathological conditions as well as to evaluate the performance of prosthesis and hearing devices, several mathematical models of the middle ear have been proposed in the literature [3]. Since Esser [4] in 1947, who studied the deformation of the TM through an analytical formulation, all mathematical models of the middle ear were developed using deterministic approaches. In contrast, experimental data of the human middle ear dynamics generally shows large discrepancies among samples. Consequently, it is still debatable the applicability of deterministic models of the middle ear once the real structure is a fuzzy system.

In this paper we use a lumped parameter model combined to Monte Carlo simulations in order to develop a probabilistic model of the human middle ear for studying its dynamic behavior uncertainties. In addition, a simplified analytical model of the outer ear is coupled to the middle ear model to expand the analysis. In the end, we aims to provide a preliminary investigation on the statistical properties of the human middle ear mechanics through a probabilistic approach.

2 METHODS

Our analysis of the middle ear's uncertainties is based on four different measures: the first three natural frequencies f_n, the frequency response of the stapes velocity by the acoustic pressure at the TM H_{fp}, the input impedance of the middle ear Z_{ME} and the wideband Energy Reflectance ER (also called as Power Reflectance). The definition of the last three measure are given as

$$H_{\mathrm{fp}} = V_{\mathrm{fp}}/P_{\mathrm{TM}}, \tag{1}$$

$$Z_{\mathrm{ME}} = P_{\mathrm{TM}}/V_{\mathrm{TM}} \tag{2}$$

and

$$ER = |R_{\mathrm{ME}}|^2, \tag{3}$$

being V_{fp} the velocity of the stapes, P_{TM} the sound pressure at the TM, V_{TM} the velocity of the TM and R_{ME} the reflection coefficient of the middle ear seen by the ear canal. These quantities were chosen to reach as mechanical measures (f_n, H_{fp} and Z_{ME}) as well as vibroacoustical measures (ER). While a pure mechanical model can be used to obtain the mechanical parameters, a vibroacoustical model is necessary to calculate ER taking account the geometry of the ear canal. Thus, the two needed approaches are described in Section 2.1 and 2.2. Lastly, Section 2.3 details the Monte Carlo simulation used in this work.

2.1 Lumped model of the middle ear

The lumped parameter model used here is based on the model proposed by Feng and Gan [5]. Our model has four degrees of freedom (DOF) related to the normal displacement of the four presented masses, neglecting the rotational movements. The masses represent the TM (m_1), malleus (m_2), incus (m_3) and the stapes (m_4). The stiffness (k_i) and dampers (c_i) with index 2, 4 and 6 represent the connection of TM and malleus and the incudomallear joint and incudostapedial joint, respectively. The stiffness and dampers with index 1, 3 and 5 represent the ligaments and tendons that hold the TM and ossicular chain in the middle ear cavity. Finally, stiffness k_7 and dampers c_7 model the cochlear load over the stapes. Figure 1(a) shows the lumped parameter model scheme.

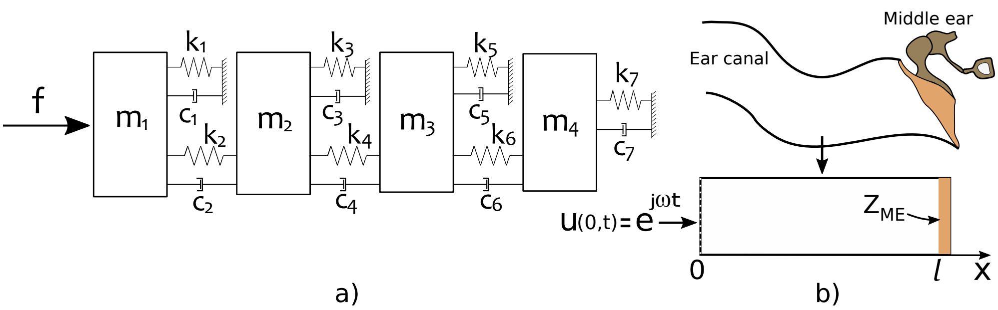

Figure 1. (a) the lumped parameter mass-spring model of the middle ear and (b) the analytical model of ear canal.

Assembling the matrices of mass **[M]**, stiffness **[K]** and damping **[C]**, the displacement of each DOF is obtained through the solution of the equation of motion

$$[\mathbf{M}]\{\ddot{x}\} + [\mathbf{C}]\{\dot{x}\} + [\mathbf{K}]\{x\} = \{f\}, \tag{4}$$

being $\{x\}^{\mathrm{T}} = \{x_1, x_2, x_3, x_4\}$ the displacement vector of all the DOFs, $\{\dot{x}\}$ and $\{\ddot{x}\}$ the time derivative of first and second order, and $\{f\}$ the excitation vector, defined as

$$\{f\}^{\mathrm{T}} = \{(A_{\mathrm{TM}} P_{\mathrm{TM}}) \quad 0 \quad 0 \quad 0\}, \tag{5}$$

being A_{TM} the TM area defined as $\pi(0.01/2)^2$ [m^2]. Note that the excitation acts only at the TM defining zero for the remaining DOFs. It should to be note that defining P_{TM}, the quantities H_{fp} and Z_{ME} can be calculated using $V_{\mathrm{TM}} = \mathrm{i}2\pi f x_1$ and $V_{\mathrm{fp}} = \mathrm{i}2\pi f x_4$, being $\mathrm{i} = \sqrt{-1}$.

To define the baseline lumped parameter model we fitted the mechanical parameters in order to match the H_{fp} from our model to one experimental data of a cadaveric temporal bone. The experimental H_{fp} was measured in a fresh temporal bone, whereas V_{fp} and P_{TM} were measured using Laser Doppler Vibrometry and a microphone with a probe tube. We carried out the experiment reproducing the procedure described by Aibara *et al.* [6]. Then, the resultant mechanical parameters fitting the theoretical-experimental H_{fp} are exposed in Table 1. The comparison of theoretical-experimental H_{fp} is shown in Figure 2(a). Also, both theoretical-experimental results are compared to the experimental mean $\pm$ standard deviation (StD) range over 11 samples experimented by Aibara *et al.* [6].

Following the fitting process of H_{fp}, we then calculated Z_{ME}. The result is shown in Figure 2(b), being the theoretical result compared to the mean $\pm$ StD range over 13 samples of cadaveric temporal bones experimented by Voss *et al.* [7]. Our result falls in the StD range up to 1 [kHz], being above the experimental range between 1 [kHz] and 4 [kHz]. Note that although we display Z_{ME} up to 10 [kHz], Voss *et al.* [7] measured only up to 4 [kHz].

Table 1. Mechanical parameters of the baseline model.

Stiffness [kN/m]	Mass [mg]	Damping [mNs/m]
k_1 = 0.2	m_1 = 2,7	c_1 = 105
k_2 = 94.7	m_2 = 35.3	c_2 = 20
k_3 = 0.96	m_3 = 35.8	c_3 = 120
k_4 = 10	m_4 = 4.4	c_4 = 66
k_5 = 0.2	-	c_5 = 30
k_6 = 10	-	c_6 = 0.28
k_7 = 1.16	-	c_7 = 124

2.2 Analytical model of ear canal

As shown in the previous section, H_{fp} and Z_{ME} can be calculated using the outcomes of the lumped parameter model. However, to calculate the *ER* taking account the length of the ear canal, an acoustical model of the ear canal is needed. Thus, we assumed the ear canal as an one dimension duct of constant cross section with an impedance Z_{ME} at the end and a velocity condition at the entrance, as shown in Figure 1(b). The acoustic pressure field in an one dimension duct can be described by

$$p(x,t) = \left(A\mathrm{e}^{\mathrm{i}kx} + B\mathrm{e}^{-\mathrm{i}kx}\right)\mathrm{e}^{\mathrm{i}2\pi f t} \tag{6}$$

being k the wave number given as $2\pi f/c_0$, c_0 the sound velocity in air and A and B the complex constants obtained from the boundary conditions. Then, the two needed boundary conditions are

$$\frac{p(l,t)}{u(l,t)} = Z_{\mathrm{ME}} \tag{7}$$

$$u(0,t) = \mathrm{e}^{\mathrm{i}2\pi f t}, \tag{8}$$

being l the length of the ear canal. We assumed $l = 32$ [mm], $c_0 = 343$ [m/s] and the air density $\rho_0 = 1.21$ [kg/m^3]. Note that the impedance Z_{ME} used as boundary condition is previously calculated with the lumped parameter model described in Section 2.1. Finally, we calculate the reflection coefficient at the end of the ear canal as $R_{\mathrm{ME}} = B/A$ and the *ER* using Equation 3. The computed *ER* is shown in Figure 2(c), where it is compared to the confidence interval (CI) of 80% measured by Shahnaz *et al.* [8] in healthy subjects. Our result of *ER* is in the CI range in almost all frequency range, being slightly out around 2 [kHz].

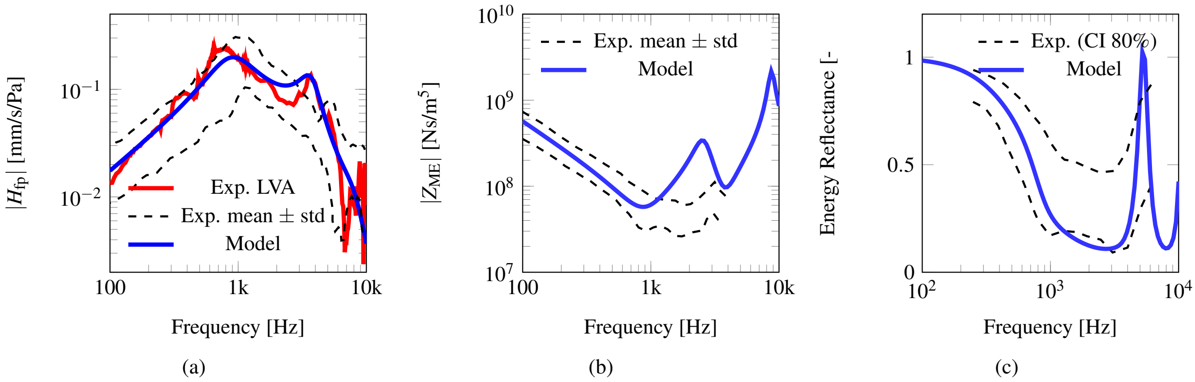

Figure 2. Magnitude of $H_{\rm fp}$ and $Z_{\rm ME}$ obtained from the lumped parameter model described in Section 2.1 and Energy Reflectance obtained from analytical model of the ear canal described in Section 2.2. Model outcomes are compared to the experimental mean ± StD from [6] in (a), [7] in (b) and [8] in (c).

Although our model provides a good results compared to the experimental references, some limitations of the model should be pointed out. Firstly, it is assumed that the TM acts as a rigid body, what is not true as observed by Cheng *et al.* [9]. Furthermore, the model is able to described only an one dimensional movement of the middle ear, also called as "piston-like movement", despite the ossicular chain presents a more complex movement in high frequencies [7]. On the other hand, the analytical model of the ear canal does not represent the ear canal curvature and variation of the cross section area.

2.3 Monte Carlo Simulation description

Monte Carlo simulation (MCS) is a probabilistic parametric method widely employed to analyze the statistical response of structures with uncertainties [10]. The procedure consists in generating n pseudo-random samples of the random variables of the system, with a given probability density functions (PDF). In what follows, the deterministic models described in Section 2.1 and 2.2 are computed for each pseudo-random sample of the ensemble, resulting in n outcomes. Finally, statistical analyzes can be made over the n results, computing the first and second statistics moments, for example.

Due the lack of experimental data of the mechanical parameters of the middle ear, some assumption on the statistical properties of them have been taken. We assumed all parameters described in Table 1 and the area of the TM ($A_{\rm TM}$) as random variables with a gaussian PDF. The mean value of each parameter is the same used in the baseline deterministic model. On the other hand, the StDs were defined as a percentage of the mean. Initially, we assumed a StD of 20% of the mean for all random variables, excepted for the $A_{\rm TM}$, whereas a StD of 12% was taken based on the De Greef *et al.* [1] observations.

In order to define a reasonable n number of pseudo-random samples, a convergence analysis was carried out. The mean and StD of the first three natural frequencies of the lumped parameter model were calculated varying the n number of samples. Figure 3 shows the convergence of the mean and StD of the first three natural frequencies for 10 up to 3000 n samples, with a step sample of 10, resulting in 299 cases computed. In addition, it is shown the mean of the means and StDs over the all computed cases. The convergence criteria were defined as ±1% of the mean of the means and ±5% for the mean of the StDs. It was observed a safe convergence for a number of samples $n \geq 1500$, where the variation of the mean for each natural frequency did not exceeded 1% of the overall mean of the means and 5% of the overall mean of the StDs.

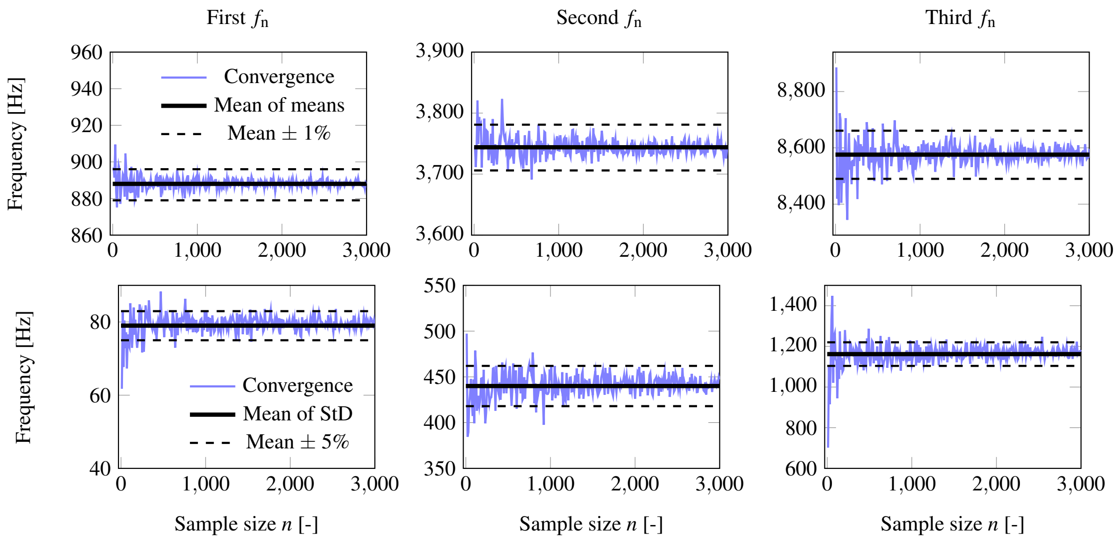

Figure 3. Convergence analysis of mean (upper panel) and standard deviation (lower panel) of the three first modes over the number of samples used in the MCS.

3 RESULTS

3.1 Dispersion of the natural frequencies f_n

To obtain the undamped natural frequencies of the system the following eigenvalue problem was solved

$$(\lambda[\mathbf{M}] - [\mathbf{K}])\Psi = 0, \tag{9}$$

begin λ the eigenvalues and Ψ the eigenvectors of the system. The natural frequencies are then calculated as $f_n = \sqrt{\lambda}/2\pi$. Then, the Equation 9 was solved for the n samples in the MCS giving n outcomes of each natural frequencies.

Figure 4 groups the results presenting the distribution of the first three natural frequencies of the system in terms of histograms. The first three natural frequencies of the system present a distribution similar to gaussian distribution. It is expected since the input parameters were statistically modeled by gaussian PDFs. For the first mode, the mean over 1500 samples is 890 [Hz] with StD of 78 [Hz], what represents 8% of the mean. On the other hand, for the second and third modes the StDs increased to 11% and 13% of the mean values, respectively. The fourth mode falls out of the frequency range of interest, being the mean equal to 32 [kHz] with a StD of almost 15% of the mean. These results suggest that the uncertainty of natural frequencies of the human middle ear increases along the frequency.

At last, it should to be noted that the natural frequencies found here are related to the one dimensional movement of ossicular chain, named in the literature as "piston-like movement". Due to the ossicular chain complexity, other resonances can be found in the in the same frequency range we analyzed. Homma *et al.* [11] observed through a 3D Finite Element model the first mode close to 1 [kHz] (similar to our result), but the second mode at 1.7 [kHz], not observed in our results.

3.2 Dispersion of the H_{fp}, Z_{ME} and ER

The measures computed with the deterministic model and exposed in Figure 2 were then computed using the MCS. Figure 5 shows the results of H_{fp}, Z_{ME} and ER by means of minimum (min) and maximum (max) values at each frequency and the mean ± StD. Also, these results are compared to experimental mean ± StD from Aibara *et al.* [6], Voss *et al.* [7] and Shahnaz *et al.* [8].

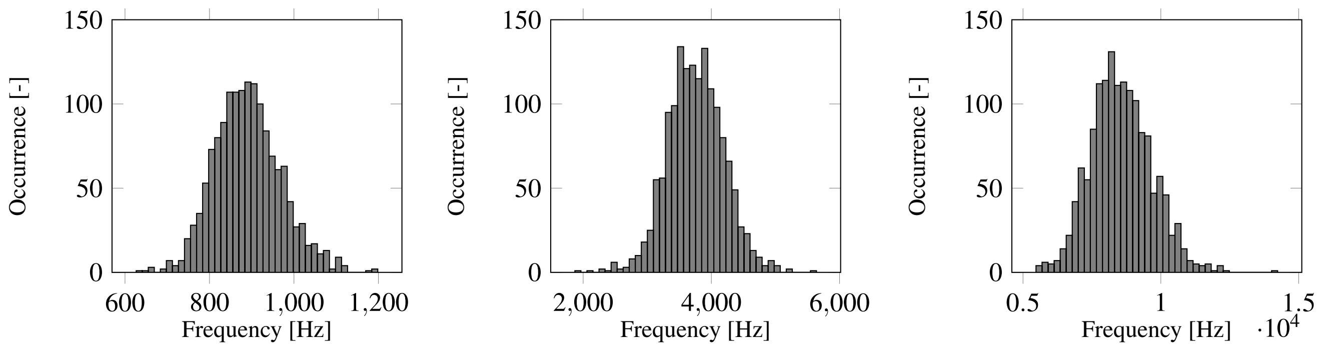

(a) Mode 1: μ=890 [Hz] and σ=78 [Hz] (b) Mode 2: μ=3755 [Hz] and σ=437 [Hz] (c) Mode 3: μ=8568 [Hz] and σ=1106 [Hz]

Figure 4. Histograms (with 40 bins each) of the first three natural frequencies of the system with $n = 1500$, being μ the mean and σ the StD. These results consider a StD of 20% of the input parameters in the MCS.

In general, the max and min results have a range larger than the experimental mean $\pm$ StD reference for the H_{fp} and Z_{ME}. However, the theoretical mean $\pm$ StD of H_{fp} is much smaller than the experimental reference. On the other hand, the theoretical mean $\pm$ StD of the Z_{ME} is comparable to the experimental reference below 1 [kHz], but has diverged from the reference above this frequency. In addition, the theoretical statistical results of the *ER* show the variation of the middle ear parameters has a minor influence on the *ER* dispersion.

Lastly, the experimental data of H_{fp}, Z_{ME} and *ER* come from different samples of temporal bones/subjects. Therefore, it is not possible to conclude what is the greater dispersion among H_{fp}, Z_{ME} and *ER* based on those experimental data.

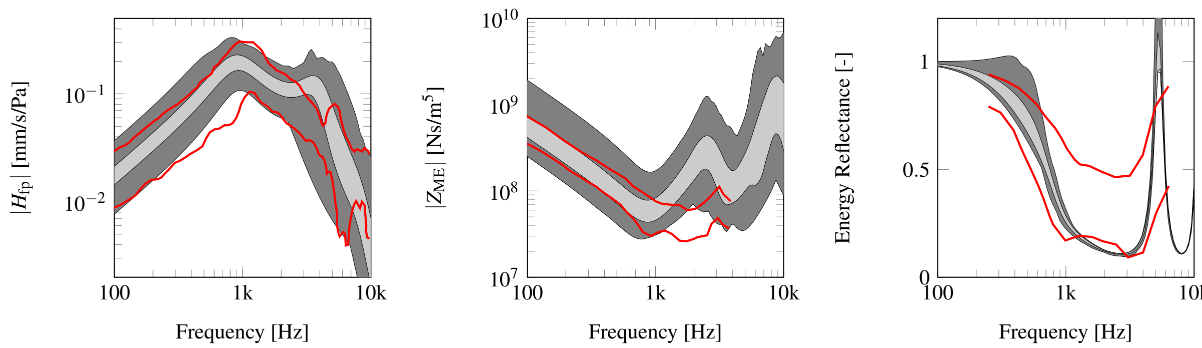

(a) (b) (c)

Figure 5. The dispersion of the $|H_{\mathrm{fp}}|$, $|Z_{\mathrm{ME}}|$ and *ER* by means of max and min values ( ) and mean $\pm$ StD ( ), being ( ) the experimental mean $\pm$ StD from [6] in (a), [7] in (b) and [8] in (c). These results consider a StD of 20% of the input parameters and $n = 1500$ in the MCS.

Once the outcomes in terms of StD of our probabilistic model showed to be considerably smaller than the experimental data, we increase the dispersion of the input parameters. Thus, the StD of the parameters which compound **[M]**, **[C]** and **[K]** were increased from 20% of the mean to 30%, 40% and 50%. Figure 6 shows the mean $\pm$ StD of the $|H_{\mathrm{fp}}|$, $|Z_{\mathrm{ME}}|$ and *ER* varying the StD of the input parameters in the MCS. The theoretical results are once more compared to the experimental data from Aibara *et al.* [6], Voss *et al.* [7] and Shahnaz *et al.* [8]. The increment of input parameters' StD from 20% up to 50% made the dispersion range of $|H_{\mathrm{fp}}|$

similar to the experimental reference below 300 [Hz] and above 2 [kHz]. On the other hand, the range of mean $\pm$ StD of $|Z_{ME}|$ diverged at high frequencies while the StD of input parameters increased. In the end, the *ER* dispersion has not presented relevant increment above 500 [Hz] increasing the StD of the input parameters.

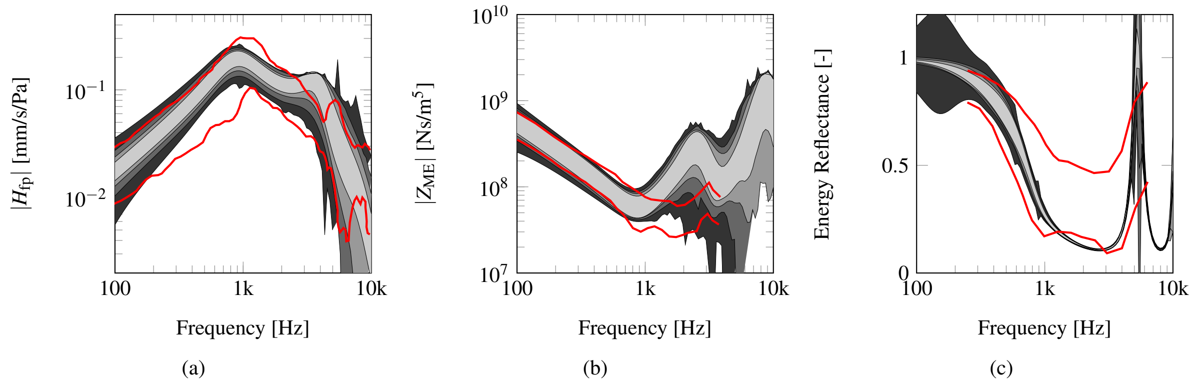

Figure 6. Mean $\pm$ StD of the $|H_{fp}|$, $|Z_{ME}|$ and *ER* varying the StD of the input parameters in the MCS, being ( ) StD of 50%, ( ) 40%, ( ) 30%, ( ) 20% and ( ) the experimental reference ([6] in (a), [7] in (b) and [8] in (c)).

4 FINAL REMARKS AND FUTURE INVESTIGATIONS

In this work we develop a model of the human middle ear using a probabilistic approach for studying middle ear uncertainties. A coupled lumped parameter and analytical model of the middle and outer ear was combined to Monte Carlo simulation and four different measures were evaluated. As expected, the first three natural frequencies of the middle ear are distributed with gaussian shape for gaussian ensembles of input parameters. Moreover, the uncertainties of the natural frequencies increase with the mode order.

In Section 3.2 we showed the model did not reproduce the dispersion of H_{fp}, Z_{ME} and *ER* seen in the experimental data assuming the StD of the input parameters as 20% of the mean with Gaussian distribution. Two hypotheses can be stated: 1. the dispersion of the input parameters was underestimated; and 2. the chosen Gaussian PDF can not be representative for one or more input parameter. The first hypothesis was tested here rising different remarks for the three measures analyzed. For the H_{fp}, the increment of input parameters' StD made the model outcomes closer to the experimental data in low and high frequencies, but not around 1 [kHz]. On the other hand, the dispersion of Z_{ME} became higher than the experimental reference above 1 [kHz] for a input parameters' StD of 40% and 50%. In other words, the increase of the input parameters' StD result in a non proportional increase of the model output's StD along the frequency. These result suggest the input parameters should hold different StD in the MCS, once we assumed the StD percentage equal for the all input parameters. Furthermore, the *ER* showed a low sensitiveness to the middle ear parameters variation. Also, *ER* grater than 1 could be seen in some cases, what is not expected. At last, our probabilistic model was based in a deterministic model fitted to one specific experimental result. This approach lead to a biased statistical result once the shape of the dispersion is similar to the deterministic case responses.

Although our probabilistic model developed in this work to study middle ear uncertainties has presented some limitations, it helped to rise some interesting questions for future investigations towards a better probabilistic approach. Therefore, some topics are intended to be assessed in the next steps, such as: 1. to use other PDF to model the distribution of the input parameters; 2. to determine the suitable StD of each input parameter separately; 3. since the present probabilistic results seemed to be biased by the deterministic model, to base the probabilistic model in more than one deterministic model; 4. to estimate experimentally the distribution of the natural frequencies; and 5. to develop a more realistic model of the ear canal considering its curvature and dissipation in order to explain the values of ER grater than 1.

Acknowledgment

The authors would like to thank CNPq (National Council for Scientific and Technological Development) and FINEP (Funding Authority for Studies and Projects) for the financial support.

REFERENCES

[1] D. De Greef, J. A. Buytaert, J. R. Aerts, L. Van Hoorebeke, M. Dierick, and J. Dirckx, "Details of human middle ear morphology based on micro-ct imaging of phosphotungstic acid stained samples," *Journal of Morphology*, vol. 276, no. 9, pp. 1025–1046, 2015.

[2] P. K. Gottlieb, Y. Vaisbuch, and S. Puria, "Human ossicular-joint flexibility transforms the peak amplitude and width of impulsive acoustic stimuli," *The Journal of the Acoustical Society of America*, vol. 143, no. 6, pp. 3418–3433, 2018.

[3] A. D. Paolis, M. Bikson, J. T. Nelson, J. A. de Ru, M. Packer, and L. Cardoso, "Analytical and numerical modeling of the hearing system: Advances towards the assessment of hearing damage," *Hearing Research*, vol. 349, pp. 111 – 128, 2017. Noise in the Military.

[4] M. H. M. Esser, "The mechanism of the middle ear: Part ii. the drum," *The bulletin of mathematical biophysics*, vol. 9, pp. 75–91, Jun 1947.

[5] B. Feng and R. Z. Gan, "Lumped parametric model of the human ear for sound transmission," *Biomechan Model Mechanobiol*, no. 3, pp. 33–47, 2004.

[6] R. Aibara, J. T. Welsh, S. Puria, and R. L. Goode, "Human middle-ear sound transfer function and cochlear input impedance," *Hearing Research*, vol. 152, no. 1, pp. 100 – 109, 2001.

[7] S. E. Voss, J. J. Rosowski, S. N. Merchant, and W. T. Peake, "Acoustic responses of the human middle ear," *Hearing Research*, vol. 150, no. 1, pp. 43 – 69, 2000.

[8] N. Shahnaz, K. Bork, L. Polka, N. Longridge, D. Bell, and B. D. Westerberg, "Energy reflectance and tympanometry in normal and otosclerotic ears," *Ear and Hearing*, vol. 30, no. 2, pp. 219–233, 2009.

[9] J. T. Cheng, M. Hamade, S. N. Merchant, J. J. Rosowski, E. Harrington, and C. Furlong, "Wave motion on the surface of the human tympanic membrane: Holographic measurement and modeling analysis," *The Journal of the Acoustical Society of America*, vol. 133, no. 2, pp. 918–937, 2013.

[10] Daouk, Sami, Louf, François, Dorival, Olivier, Champaney, Laurent, and Audebert, Sylvie, "Uncertainties in structural dynamics: overview and comparative analysis of methods," *Mechanics & Industry*, vol. 16, no. 4, p. 404, 2015.

[11] K. Homma, Y. Du, Y. Shimizu, and S. Puria, "Ossicular resonance modes of the human middle ear for bone and air conduction," *The Journal of the Acoustical Society of America*, vol. 125, no. 2, pp. 968–979, 2009.